Crystal structure and magnetic behaviour of a two-dimensional step-shaped cyano-bridged complex [Cu(dien)]₃[Fe(CN)₆]₂·6H₂O (dien = diethylenetriamine) †

Hui-Zhong Kou,[a] Dai-Zheng Liao,*,[a] Peng Cheng,[a] Zong-Hui Jiang,[a] Shi-Ping Yan,[a] Geng-Lin Wang,[a] Xin-Kan Yao[b] and Hong-Gen Wang[b]

[a]Department of Chemistry, Nankai University, Tianjin, 300071, P. R. China
[b]Central Laboratory, Nankai University, Tianjin, 300071, P. R. China

A bimetallic compound [Cu(dien)]₃[Fe(CN)₆]₂·6H₂O (dien = diethylenetriamine) has been prepared and its crystal structure determined: space group $P2_1/a$, $a = 14.896(3)$, $b = 14.128(5)$, $c = 20.267(6)$ Å, $\beta = 96.31(3)°$ and $Z = 4$. The structure consists of a one-dimensional chain of {[Cu(dien)]₂[Fe(CN)₆]}⁺ cations and binuclear {[Cu(dien)(H₂O)][Fe(CN)₆]}⁻ moieties bridged by one CN⁻ ligand of the [Fe(CN)₆]³⁻ anion. The chains are linked by hydrogen bonds giving rise to a unique step-shaped two-dimensional network. In the crystal all the copper(II) ions have a distorted square-based-pyramidal geometry. From magnetic susceptibility measurements the complex was found to exhibit a weak ferromagnetic interaction between the copper(II) and iron(III) atoms.

Molecular magnetism is a new field of research which has emerged over the past decade or so.[1] The synthesis of well characterized molecular-based magnets with Curie temperatures, T_c, close to room temperature remains a challenge.[2–5] Until now, several systems of ferromagnets have been described with critical temperatures ranging from 0.6 to 450 K.[3,6–21] Among them, the cyanide system based on Prussian Blue, is particularly useful, and its magnetic properties have attracted much interest.[16,21]

Since copper(II) normally possesses four-, five- or six-coordination, it was anticipated that the coupling of a copper amine complex to [Fe^{III}(CN)₆]³⁻ ion might enable the formation of a novel family of magnetic compounds with potential control over the structure of the crystal lattice. We therefore examined the reaction of [Cu(dien)(H₂O)₂]Cl₂ (dien = diethylenetriamine) and K₃[Fe(CN)₆]. The product easily crystallized, [Cu(dien)]₃[Fe(CN)₆]₂·6H₂O, has a unique two-dimensional structure and exhibits special magnetic behaviour.

Experimental

Materials

The compounds K₃[Fe(CN)₆], CuCl₂·2H₂O and dien were of analytical grade (Peking Chemical Company).

Synthesis of [Cu(dien)]₃[Fe(CN)₆]₂·6H₂O

To an aqueous solution of [Cu(dien)(H₂O)₂]Cl₂ (0.2 mmol, 5 cm³), previously prepared by mixing CuCl₂·2H₂O (0.2 mmol, 34.1 mg) and dien (0.2 mmol, 0.022 cm³) in water (5 cm³), was added K₃[Fe(CN)₆] (0.2 mmol, 65.8 mg) in water (5 cm³) with stirring at room temperature. The precipitate thus produced was filtered off and washed several times with water (10 cm³). Recrystallization from hot water gave microcrystals, which were filtered off and dried in a desiccator over CaCl₂. The elemental analysis results (Found C, 28.5; H, 4.8; N, 28.3. C₂₄H₅₁Cu₃Fe₂N₂₁O₆ requires C, 28.0; H, 5.0; N, 28.5%) were in agreement with the formula of the sample used for X-ray analysis. The water content was determined by TGA. A loss of 10.1% in the temperature range 40–110 °C was consistent with the presence of six water molecules per formula unit. The density of the

complex was measured by the flotation method (carbon tetrachloride and dibromomethane), $D_m = 1.60(1)$ Mg m⁻³ and agreed with calculated value ($D_c = 1.617$ Mg m⁻³).

Crystals adequate for X-ray analysis were obtained by slow evaporation of the above filtrate.

Physical measurements

Infrared spectra were monitored (in the 4000–400 cm⁻¹ region) with a Nicolet 5DX FT-IR spectrophotometer using KBr pellets. Thermogravimetric analyses were carried out with a Dupont model 1090B derivatograph. Magnetic susceptibility data for a powder sample were collected in the temperature range 1.5–300 K with a Model CF-1 vibrating-sample magnetometer at an applied field of 1 T.
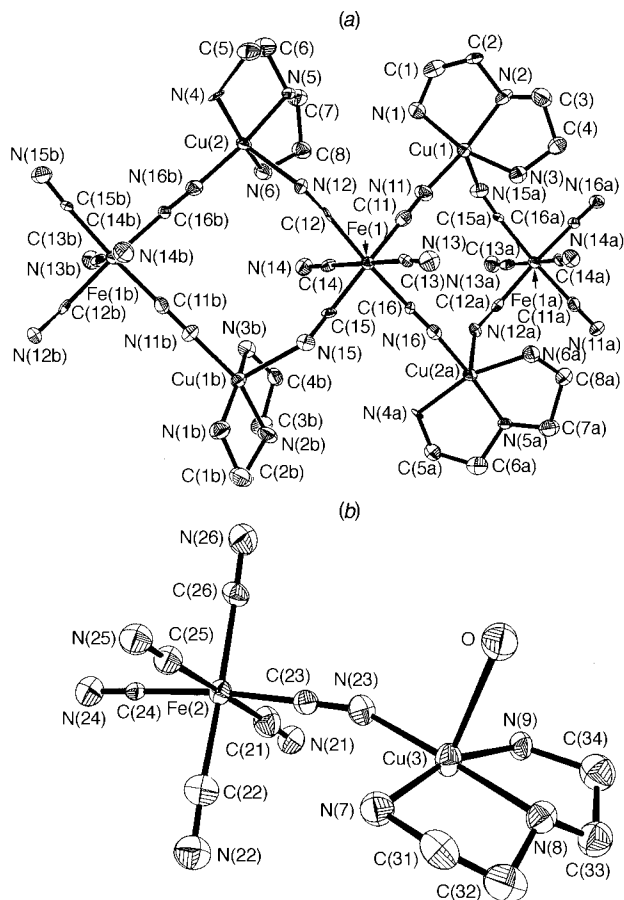
Crystallography

A dark blue block of [Cu(dien)]₃[Fe(CN)₆]₂·6H₂O was sealed in a glass capillary. Diffraction experiments were performed with graphite-monochromated Mo-Kα radiation ($\lambda = 0.710\,73$ Å) on an Enraf-Nonius CAD-4 diffractometer; 5086 independent reflections were collected in the range θ 7.68–12.06° by the ω–2θ scan technique with a scan speed of 0.92–5.49° min⁻¹ at 299 ± 1 K, of which 2524 reflections [$I \geqslant 3\sigma(I)$] were considered observed and used for the structure refinements. Details of the crystal data, collection and refinement are listed in Table 1. Intensity data were corrected for Lorentz-polarization factors. The observed extinctions were consistent with the space group $P2_1/a$. Three standard reflections were recorded every 1 h. Their intensities showed no variation over the duration of data collection. All non-hydrogen atoms were located using direct methods and subsequently Fourier and Fourier-difference syntheses. The final refinement (based on F^2) by full-matrix least squares with anisotropic thermal parameters for the non-hydrogen atoms converged with R and R' factors of 0.059 and 0.067, respectively (unit weights for all observed reflections). Hydrogen atoms were refined with fixed position parameters and fixed isotropic thermal parameters. The final difference map revealed no peaks of chemical significance (maximum 0.89 and minimum −0.52 e Å⁻³).

All calculations were performed on a PDP11/44 computer using the SDP-PLUS program system.[23]

Atomic coordinates, thermal parameters, and bond lengths

† Non-SI unit employed: $\mu_B \approx 9.27 \times 10^{-24}$ J T⁻¹.

Fig. 1 The ORTEP[24] drawings of (*a*) the infinite units and (*b*) the binuclear unit, showing the atom numbering schemes

and angles have been deposited at the Cambridge Crystallographic Data Centre (CCDC). See Instructions for Authors, *J. Chem. Soc., Dalton Trans.*, 1997, Issue 1. Any request to the CCDC for this material should quote the full literature citation and the reference number 186/445.

Results and Discussion

Crystal Structure

Selected bond distances and angles are shown in Table 2. The structure (Fig. 1) consists of a one-dimensional array of {[Cu-(dien)]$_2$[Fe(CN)$_6$]}$^+$ units bridged by four CN$^-$ ligands of each [Fe(CN)$_6$]$^{3-}$ anion and binuclear {[Cu(dien)(H$_2$O)-Fe(CN)$_6$]}$^-$ units, formed by the union of the [Cu(dien)(H$_2$O)]$^{2+}$ cation and [Fe(CN)$_6$]$^{3-}$ anion through one bridging CN$^-$ ligand. The infinite chain structure is clearly seen in Fig. 2. The co-ordination environment of Cu^{2+} in the chain can be described as distorted square-based pyramidal, with the three nitrogen atoms of the dien ligand and one nitrogen atom of one CN$^-$ bridging ligand [Cu(1)–N(11) 1.99, Cu(2)–N(16b) 1.97 Å] in the equatorial plane and the nitrogen atom of another CN ligand [Cu(1)–N(15a) 2.28, Cu(2)–N(12) 2.32 Å] in the axial position. The largest deviations from the least-squares plane for Cu(1) through N(1),N(2),N(3),N(11) and for Cu(2) through N(4),N(5),N(6),N(16) are −0.024 Å at N(2) and −0.09 Å at N(5), respectively. The Cu(1) atom lies 0.321 Å out of its basal plane toward the apical site and Cu(2) is displaced out of the equatorial plane away from the axial N(12) atom by 0.219 Å. The building block [Fe(CN)$_6$]$^{3-}$ assumes an octahedrally co-ordinated geometry with six CN$^-$ groups and the Fe–C bond lengths ranging from 1.89 to 1.95 Å where each of the equatorial CN$^-$ ligands co-ordinates to a Cu atom from a Cu(dien) moiety and the others are terminal. Not all of the four bridging cyanide groups, however, behave in the same way: two
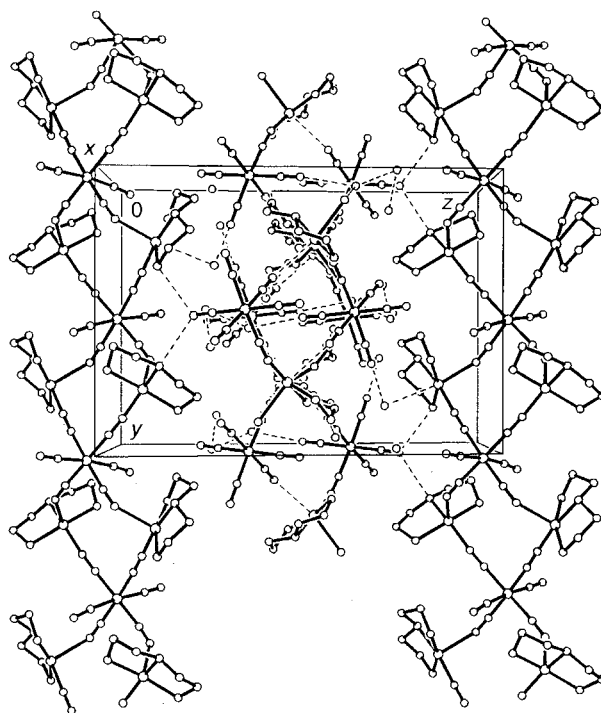
Fig. 2 Projection of the polymeric chain structure along the *z* axis

of them, namely C(12)≡N(12) and C(15)≡N(15), give non-linear Fe–C≡N–Cu sequences, the Cu(1b)–N(15)–C(15) and Cu(2)–N(12)–C(12) angles being *ca.* 142 and 138.7°, respectively; the other two, namely C(11)≡N(11) and C(16)≡N(16), are almost linearly bonded to the adjacent copper atoms, the Cu(1)–N(11)–C(11) and Cu(2a)–N(16)–C(16) angles being *ca.* 174 and 176°, respectively. In the Cu–Fe binuclear units the copper atoms also have a distorted square-based pyramidal geometry of which the equatorial plane is defined by the three nitrogens of dien and the N(23) of a CN$^-$ ligand [Cu(3)–N(23) 1.96 Å]. The oxygen atom of one water molecule co-ordinates axially to the copper centre [Cu–O 2.43 Å]. The largest deviation from the least-squares plane for Cu(3) through N(7),N(8),N(9),N(23) is −0.10 Å at N(8). The Cu(3) atom lies 0.114 Å out of its basal plane away from the axial O atom. The bond lengths and angles within each [Cu(dien)]$^{2+}$ unit do not differ significantly from values reported previously.[25]

In the crystal the chains linked by N(13a)···N(5m) and N(12j)···N(3) hydrogen bonds (Fig. 3) align along the *xy* plane to form a two-dimensional layer structure. Table 3 shows the intermolecular contacts. The lattice water molecules are situated between the layers. The adjacent chains are staggered a little, giving rise to a novel step-shaped structure. The seemingly discrete Cu–Fe binuclear units are practically not isolated but linked into layers through N(25)···N(2) and N(25b)···N(4a) hydrogen bonds, forming a unique structure. The copper–iron separations within the chains are 5.034 Å for Fe(1)···Cu(1) and 5.011 Å for Fe(1)···Cu(2), and in the binuclear units Fe(2)···Cu(3) is 4.949 Å. The nearest interchain Fe(1)···Cu(1) and Fe(1)···Cu(2) separations in the layer are 5.003 and 5.025 Å, respectively. The Fe···Fe distance within the chain is 7.325 Å, and the nearest interchain Fe···Fe separation is 6.32 Å.

Infrared spectra

The IR spectrum of [Cu(dien)]$_3$[Fe(CN)$_6$]$_2$·6H$_2$O in the crystalline sample shows two strong bands at 2128 and 2176 cm^{-1} and a broad shoulder at *ca.* 2112 cm^{-1} which are attributed to C≡N stretching modes. The shift of ν(C≡N) to higher wavenumber compared with that of K$_3$[Fe(CN)$_6$] is consistent with the formation of C≡N bridges as revealed by the X-ray determin-

Table 1 Crystallographic data and data-collection parameters for the complex

Formula	$C_{24}H_{51}Cu_3Fe_2N_{21}O_6$
M	1032.13
Crystal system	Monoclinic
Space group	$P2_1/a$
$a/Å$	14.896(3)
$b/Å$	14.128(5)
$c/Å$	20.267(6)
$\beta/°$	96.31(3)
$U/Å^3$	4239(5)
Z	4
$D_c/Mg\ m^{-3}$	1.617
Crystal dimensions/mm	$0.3 \times 0.1 \times 0.4$
μ/mm^{-1}	2.215
Absorption correction applied	Empirical [22]
Transmission factors: minimum, maximum	0.651, 1.338
h, k, l Limits	-15 to 15, 0–14, 0–21
$F(000)$	2116
p Factor used in weighting	1 for all observed reflections
Data collected	5434
Unique data	5086
Data with $I \geqslant 3\sigma(I)$	2524
Agreement factor (on I)	0.10
No. variables	521
Largest shift/e.s.d. in final cycle	0.20
R^a	0.059
R'^b	0.067
Goodness of fit ^{c}	1.636

$^a \Sigma||F_o|^2 - |F_c|^2|/\Sigma|F_o|^2$. $^b [\Sigma w(|F_o|^2 - |F_c|^2)^2/\Sigma w|F_o|^2]^{\frac{1}{2}}$; $w = 1/[\sigma^2(F_o) + (0.020F_o)^2 + 1.000]\cdot F_o$. $^c [\Sigma w(|F_o - F_c|)^2/(N_{obs} - N_{para})]^{\frac{1}{2}}$.

Table 2 Selected bond distances (Å) and angles (°)

Cu(1)–N(1)	2.03(2)	Cu(1)–N(2)	2.02(1)
Cu(1)–N(3)	2.04(1)	Cu(1)–N(11)	1.99(1)
Cu(1)–N(15a)	2.28(1)	Cu(2)–N(4)	2.01(1)
Cu(2)–N(5)	2.027(9)	Cu(2)–N(6)	2.03(2)
Cu(2)–N(16b)	1.97(1)	Cu(3)–N(7)	2.02(1)
Cu(3)–N(8)	2.01(2)	Cu(3)–N(9)	2.04(2)
Cu(3)–N(23)	1.96(1)	Cu(3)–O	2.43(1)
Fe(1)–C(11)	1.89(1)	Fe(1)–C(12)	1.94(1)
Fe(1)–C(13)	1.95(1)	Fe(1)–C(14)	1.91(1)
Fe(1)–C(15)	1.95(1)	Fe(1)–C(16)	1.93(1)
Fe(2)–C(21)	1.95(2)	Fe(2)–C(22)	1.91(2)
Fe(2)–C(23)	1.92(2)	Fe(2)–C(24)	1.91(1)
Fe(2)–C(25)	1.94(2)	Fe(2)–C(26)	1.93(1)
Cu(1)–N(11)–C(11)	174(2)	Cu(1)–N(15a)–C(15a)	142(2)
Cu(2)–N(12)–C(12)	138(1)	Cu(2)–N(16a)–C(16a)	176(2)
Cu(3)–N(23)–C(23)	163(1)		

Symmetry operations: a $\frac{1}{2} - x$, $\frac{1}{2} + y$, $2 - z$, b $\frac{1}{2} - x$, $-\frac{1}{2} + y$, $2 - z$.

Table 3 Intermolecular contacts (Å)

|			
N(25)···N(2)	2.892	N(12j)···N(3)	2.968
N(25b)···N(4a)	2.999	N(13a)···N(5m)	2.969

Symmetry operations: a $\frac{1}{2} - x$, $\frac{1}{2} + y$, $2 - z$, b $\frac{1}{2} - x$, $-\frac{1}{2} + y$, $2 - z$, j $-x$, $-y$, $2 - z$, m $\frac{1}{2} + x$, $\frac{1}{2} - y$, z.

Fig. 3 (*a*) Projection of the two-dimensional layer structure along the *xy* plane. (*b*) View of interchain interactions among the unique chains through hydrogen bonds (- - -)
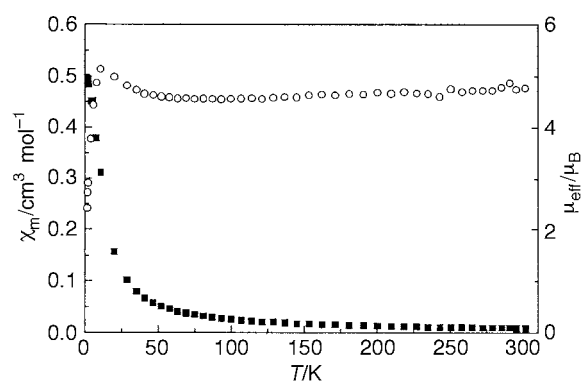
Fig. 4 Temperature dependence of χ_m (■) and μ_{eff} (○) for $[Cu(dien)]_3[Fe(CN)_6]_2\cdot6H_2O$

ation. The shoulder is due to the terminal CN stretching vibration. The IR spectrum of a powder sample of $[Cu(dien)]_3$-$[Fe(CN)_6]_2\cdot6H_2O$ is the same as that of the crystalline sample.

Magnetic properties

The magnetic properties of a powder sample of $[Cu(dien)]_3$-$[Fe(CN)_6]_2\cdot6H_2O$ are represented in the form of the χ_m *vs. T* and μ_{eff} *vs. T* plots in Fig. 4, χ_m being the molar magnetic susceptibility and μ_{eff} the effective magnetic moment. At room temperature, the effective magnetic moments of $[Cu(dien)-(H_2O)_2]Cl_2$ and $K_3[Fe(CN)_6]$ are 1.86 and 2.37 μ_B,[26] while the μ_{eff} value of the present complex is 4.75 μ_B, which is essentially equal to $(3\ \mu_{eff}^2\{[Cu(dien)(H_2O)_2]Cl_2\} + 2\ \mu_{eff}^2\{K_3[Fe(CN)_6]\})^{\frac{1}{2}}$. As the temperature is lowered, μ_{eff} is almost constant until around 63 K, then increases smoothly as *T* is lowered further. At around 10.6 K μ_{eff} reaches a maximum of 5.13 μ_B and then decreases sharply reaching a value of 2.42 μ_B at 1.48 K. Such magnetic behaviour is characteristic of dominant ferromagnetic interactions upon which weak antiferromagnetic interactions are superimposed.[27]

The ferromagnetic interaction between the iron(III) and copper(II) ions can be rationalized in terms of the strict orthogonality of the magnetic orbitals of these low-spin ions. According to the crystal structure and ligand-field theory, a copper(II) ion in square-pyramidal surroundings has one unpaired electron in a $d_{x^2-y^2}$ orbital [28] (*x* and *y* axes are taken along the donor atoms) which interacts with the molecular orbitals of the cyano bridge having the same symmetry, pro-
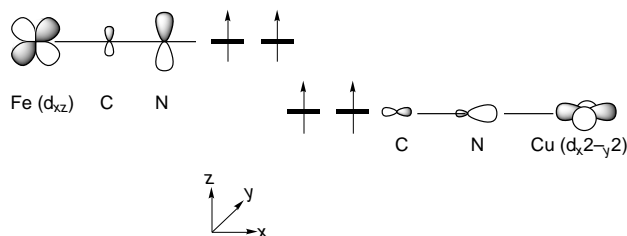
Fig. 5 Orthogonality between d_{xz} iron(III) and $d_{x^2-y^2}$ copper(II) magnetic orbitals in $[Cu(dien)]_3[Fe(CN)_6]_2 \cdot 6H_2O$

ducing a magnetic orbital with σ character. A low-spin iron(III) ion in octahedral surroundings has unpaired electron density in d_{xy}, d_{xz} and d_{yz} orbitals which interact with other molecular orbitals of the cyano bridge having appropriate symmetry, producing a magnetic orbital with π character. Consequently, strict orthogonality is obeyed and the interaction between Cu[II] and Fe[III] should be ferromagnetic (see Fig. 5). Quantitatively, the interactions between nearest neighbours are very weak. This might be due to the large distance between the magnetic ions and the bent Fe−C≡N−Cu bonds. Therefore, more examples with such kinds of interactions are needed to clarify the mechanism.

The abrupt decrease in the magnetic moment below 10.6 K may result from an intermolecular antiferromagnetic interaction. It is noteworthy that adjacent chains in the crystal are quite near to each other, which may lead to a three-dimensional antiferromagnetic ordering at low temperature through hydrogen bonds.

Conclusion

An extended copper(II)–iron(III) structure has been obtained from the reaction of the $[Cu(dien)(H_2O)_2]^{2+}$ cation and the $[Fe(CN)_6]^{3-}$ anion. The assembly of the two components is achieved through the bridging mode of the CN^- ligand and is also due to the co-ordination properties of the copper ion. On comparing the magnetic behaviour of our complex with that of $[Cu(en)]_3[Fe(CN)_6]_2 \cdot 3H_2O$ (en = ethane-1,2-diamine) reported previously [6] which shows ferromagnetic behaviour with a phase transition at *ca.* 30 K, we discover that there is a significant difference between the two complexes with similar formula. It is likely that the difference in magnetic behaviour is a consequence of the changes in assembly mode. In order to obtain a correlation between the magnetic properties and assembly structure more examples of this kind of complex are needed. Further work along these lines is in progress.

Acknowledgements

References

1 O. Kahn, *Molecular Magnetism*, VCH, New York, 1993.
2 O. Kahn, *Molecular Magnetic Materials*, eds. D. Gatteschi, O. Kahn, J. S. Miller and F. Palacio, NATO ASI Series E, Kluwer, Dordrecht, 1991, vol. 198, p. 35.
3 J. M. Manriquez, G. T. Yee, R. S. Mclean, A. J. Epstein and J. S. Miller, *Science*, 1991, **252**, 1415.
4 W. D. Griebler and D. Babel, *Z. Naturforsch., Teil B*, 1982, **87**, 832.
5 P. M. Allemand, K. C. Khemani, A. Koch, F. Wudl, K. Holczer, S. Donovan, G. Grüner and J. D. Thompson, *Science*, 1991, **253**, 301.
6 H. Z. Kou, D. Z. Liao, P. Cheng, Z. H. Jiang and G. L. Wang, *Transition Met. Chem.*, 1996, **21**, 349.
7 J. S. Miller, Y. Pei, M. Verdaguer and O. Kahn, *J. Am. Chem. Soc.*, 1987, **108**, 7428.
8 O. Kahn, Y. Pei, M. Verdaguer, J. P. Renard and J. Sletten, *J. Am. Chem. Soc.*, 1988, **110**, 782.
9 A. Caneschi, D. Gatteschi, J. P. Renard, P. Rey and R. Sessoli, *Inorg. Chem.*, 1989, **28**, 1976.
10 K. Nakatani, J. Y. Carriat, Y. Jouraux, O. Kahn, F. Lloret, J. P. Renard, J. Sletten and M. Verdaguer, *J. Am. Chem. Soc.*, 1989, **111**, 5739.
11 K. Nakatani, D. Bergerat, E. Codjovi, C. Mathoniere, Y. Pei and O. Kahn, *Inorg. Chem.*, 1991, **30**, 3977.
12 Y. Pei, O. Kahn, K. Nakatani, E. Codjovi, C. Mathoniere and T. Sletten, *J. Am. Chem. Soc.*, 1991, **113**, 6558.
13 H. Tamaki, Z. J. Zhong. N. Matsumoto, S. Kida, M. Kcikawa, N. Achiwa and Y. Hashimoto, *J. Am. Chem. Soc.*, 1992, **114**, 6974.
14 V. Gadet, T. Mallah, I. Castro and M. Verdaguer, *J. Am. Chem. Soc.*, 1992, **114**, 9213.
15 H. O. Stumpf, L. Ouahab, Y. Pei, D. Grandjean and O. Kahn, *Science*, 1993, **261**, 447.
16 T. Mallah, S. Thiebaut, M. Verdaguer and P. Veillet, *Science*, 1993, **262**, 1554.
17 S. Decurtins, H. W. Schmalle and H. R. Oswald, *Inorg. Chim. Acta*, 1994, **216**, 65.
18 W. R. Entley and G. S. Girolami, *Science*, 1995, **268**, 397.
19 H. Miyasaka, N. Matsumoto, H. Okawa, N. Re, E. Gallo and C. Floriani, *J. Am. Chem. Soc.*, 1996, **118**, 981.
20 M. Ohba, N. Maruone, H. Okawa, T. Enoki and J.-M. Latour, *J. Am. Chem. Soc.*, 1994, **116**, 11566.
21 V. Gadet, M. B. Doeutt, L. Force, M. Verdaguer, K. ElMalkhi, A. Deroy, J. P. Besse, C. Chapperi, P. Veillet, J. P. Renare and P. Beauvillam, *Molecular Magnetic Materials*, eds. D. Gatteschi, O. Kahn, J. S. Miller and F. Palacio, NATO ASI Series 198, Kluwer, Dordrecht, 1990, p. 281.
22 N. Walker and D. Stuart, DIFABS, *Acta Crystallogr., Sect. A*, 1983, **39**, 158.
23 SDP-PLUS, Enraf-Nonius, Delft, 1985.
24 C. K. Johnson, ORTEP, Report ORNL-5138, Oak Ridge National Laboratory, Oak Ridge, TN, 1976.
25 G. O. Morpurgo, V. Mosini, P. Porta, G. Dessy and V. Fares, *J. Chem. Soc., Dalton Trans.*, 1980, 1272.
26 I. Bertini, C. Luchinat, F. Mani and A. Scozzafava, *Inorg. Chem.*, 1980, **19**, 1333.
27 C. Michaut, L. Ouahab, P. Bergerat, O. Kahn and A. Bousseksou, *J. Am. Chem. Soc.*, 1996, **113**, 3610.
28 B. J. Hathaway and D. E. Billing, *Coord. Chem. Rev.*, 1970, **5**, 143.